

Photochromism of a Diarylethene Having an Azulene Ring

Jun-ichiro Kitai,[†] Takao Kobayashi,^{*,‡} Waka Uchida,[§] Makoto Hatakeyama,[§] Satoshi Yokojima,^{||,⊥} Shinichiro Nakamura,^{*,⊥} and Kingo Uchida^{*,†}

[†]Department of Materials Chemistry, Faculty of Science and Technology, Ryukoku University, Seta, Otsu 520-2194, Japan

[‡]Mitsubishi Chemical Group, Science and Technology Research Center, Inc., 1000 Kamoshida, Yokohama 227-8502, Japan

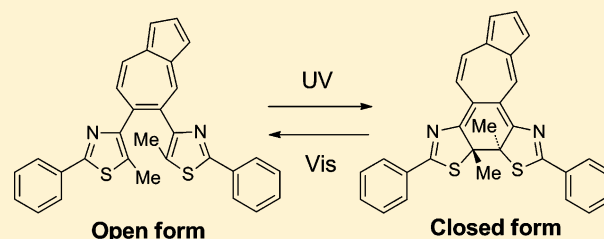
[§]Department of Biomolecular Engineering, Tokyo Institute of Technology, Nagatsuta, Midori-ku, Yokohama 226-8503, Japan

^{||}Tokyo University of Pharmacy and Life Sciences, 1432-1 Horinouchi, Hachioji, Tokyo 192-0392, Japan

[⊥]Nakamura Laboratory, RIKEN Research Cluster for Innovation, 2-1 Hirosawa, Wako, Saitama 351-0198, Japan

S Supporting Information

ABSTRACT: Diarylethene derivatives incorporating an azulene ring at the ethene moiety were synthesized. One derivative having thiazole rings showed the expected coloration reaction by excitation at 313 nm (to a higher singlet state) but not when excited at 635 nm (S_0 to S_1 excitation). The system demonstrates that the cyclization reaction can be controlled by selective excitation at different wavelengths of the absorption spectrum. On the other hand, another derivative having thiophene rings did not show any photochromism. The results clearly show the importance of the coplanarity of the system for the photoisomerization.



■ INTRODUCTION

Recently, the photoresponsive system in which a photochromic molecule is combined with the other chromophores has been paid much attention from the viewpoint of novel photo-switchable systems.¹ More than 100 years have passed since azulene was first isolated by Piesse from the distillation of chamomile oil. Azulenes constitute the most well-known class of polycyclic nonbenzenoid aromatic compounds with their unusual electronic structure and remarkable colors.² The blue color is due to absorption from the S_0 to the S_1 state. Azulene shows an extremely weak “normal” $S_1 \rightarrow S_0$ fluorescence and a significant “anomalous” $S_2 \rightarrow S_0$ fluorescence, which violates Kasha’s rule³ for emission. There have been several studies⁴ on the photophysics of azulene and the mechanism of the anomalous fluorescence is well understood. The lack of normal fluorescence from S_1 reflects the very fast nonradiative decay from S_1 to S_0 (the short lifetime of the S_1 state of azulene has been experimentally and theoretically confirmed), and the observation of significant fluorescence from S_2 is due to the slow internal conversion from S_2 to S_1 , caused by the relatively large energy gap between S_2 and S_1 .

In the field of photochromism, Tokumaru et al. introduced the azulene ring as one of the aromatic rings of a photochromic azobenzene, which underwent *cis* to *trans* one-way isomerization on a triplet manifold.⁵ However, the specific excited states were not well applied in the photochromism. In the family of photochromic compounds, diarylethenes have excellent photochromic properties with high thermal stability of both isomers and a high fatigue resistant under multiple photochromic switching cycles.⁶ Here, they obey Kasha’s rule;

thus, their photoreactivity is independent of the wavelength of the incident light. Over the past decade, Miyasaka et al. observed the extraordinarily high efficient cycloreversion (ring-opening) reaction of a diarylethene by the multiphoton excitation using a pulsed laser at high photon densities. They concluded that the orbital parentage of the electronic state plays an important role in the enhancement of the cycloreversion reaction.⁷

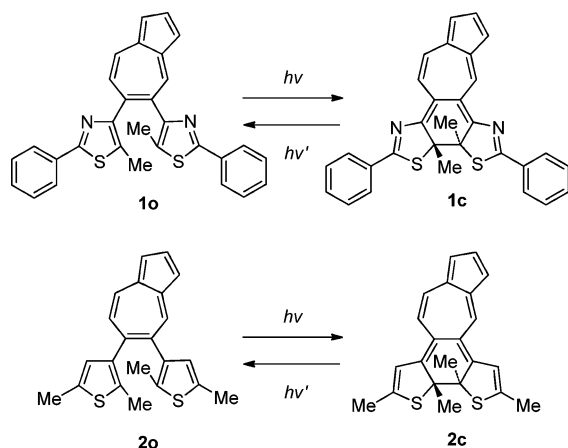
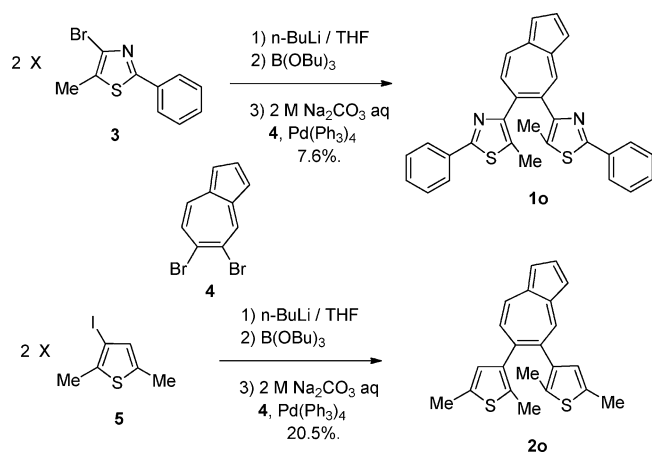
Here, we have designed new diarylethene derivatives with an azulene ring fused to the ethene moiety in which the reactivity of the cyclization (ring-closing) reaction of the diarylethene can be controlled by tuning the wavelength of irradiation without the need for high peak power pulsed excitation. Because the absorption spectra of the open-ring isomers should be composed of the absorption of the azulene ring and the aryl rings, comparison of UV and visible light excitation for cyclization of the open-ring isomer is interesting to examine. Such a molecular design in which a photophysically active unit was introduced to a diarylethene to deliver multiple-functionality has been described before for example in a stilbene diarylethene system;⁸ however, in that case a complete loss of the photoreactivity of one of the units was observed.

■ RESULTS AND DISCUSSION

Diarylethenes **1o** and **2o** (Scheme 1) were newly synthesized by the Suzuki coupling between five-membered aryl halides and 5,6-dibromoazulene which is prepared by Lemal’s method.⁹

Received: January 7, 2012

Published: March 12, 2012

Scheme 1. Photochromic Reaction of Diarylethenes **1** and **2**Scheme 2. Synthetic Procedure of Derivatives **1o** and **2o**

The route is shown in Scheme 2. The derivative **1o** showed the photochromism in hexane solution as well as the other derivatives having thiazole rings as aryl groups,¹⁰ and the spectral changes are shown in Figure 1a. Diarylene **1o** has two absorption bands; a smaller band corresponding to S_0 to S_1 excitation of the azulene ring was observed at 594 nm (ϵ 1.0×10^3 M⁻¹ cm⁻¹), and an intense band corresponding to a S_0 to a higher level singlet state excitation was observed at 288 nm (ϵ 9.5×10^4 M⁻¹ cm⁻¹). Because of the S_0 to S_1 excitation band of the azulene ring, the color of the hexane solution of **1o** was blue. Upon UV (313 nm) irradiation, new absorption bands at 495 nm (ϵ 1.6×10^4 M⁻¹ cm⁻¹) and around 700 nm appeared (broken line in Figure 1a), and the color changed to brownish pink. The bands disappeared upon irradiation with visible light ($\lambda > 500$ nm) and regenerated the original spectra, as shown in the solid line in Figure 1a. To ascertain that the new bands were attributed to the closed-ring isomer **1c**, the photoreaction was monitored by ¹H NMR spectroscopy.¹¹ Before UV irradiation, the two methyl signals of **1o** were observed at 2.25 and 2.29 ppm. After UV irradiation, two new methyl signals appeared at 2.11 and 2.15 ppm and disappeared upon irradiation with visible light (Figure S1, Supporting Information). Compound **1c** was thermally stable in hexane solution at room temperature for 24 h but reverted to **1o** with a half-life of 13 h at 70 °C in the dark. The activation energy for the thermal cycloreversion was 82.8 kJ/mol (Figure S2, Supporting Information).

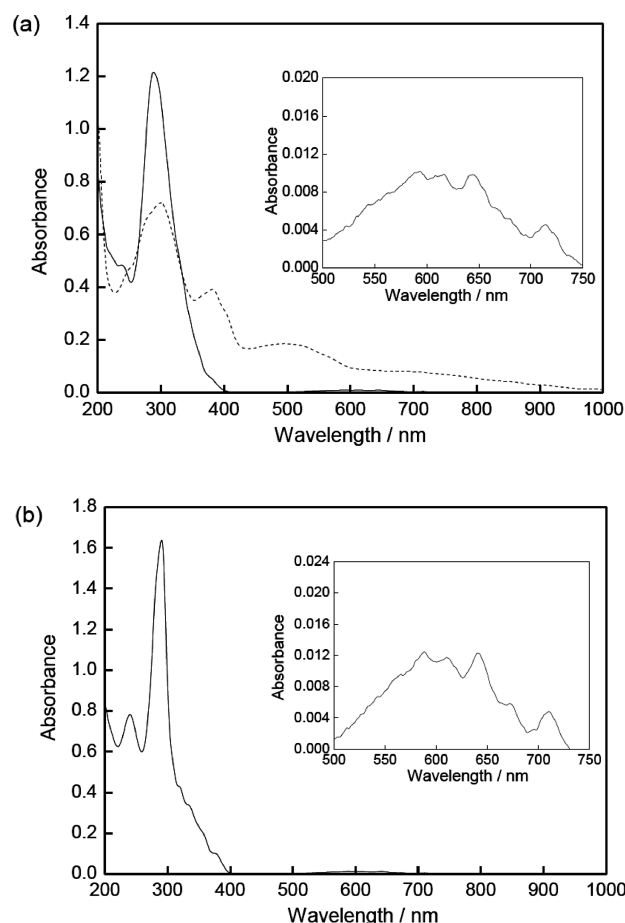


Figure 1. (a) Photoinduced spectral changes of diarylene **1** in hexane (1.3×10^{-5} M). Inset shows absorption spectrum of **1o** in the 500–750 nm range. Solid line: before UV irradiation. Broken line: after 313 nm UV irradiation for 16 min ($1o/1c = 13:87$). (b) Absorption spectrum of **2o** in hexane.

The absorption spectrum of **2o** in hexane is shown in Figure 1b. Diarylene **2o** has also two absorption bands; the smaller structured band is observed around 594 nm (ϵ 1.0×10^3 M⁻¹ cm⁻¹), which is assigned to the S_0 to S_1 excitation of azulene ring, and another intense band is observed at 290 nm (ϵ 9.5×10^4 M⁻¹ cm⁻¹), which is attributed to the excitation from S_0 to the higher excited singlet state of the molecule. No absorption spectral changes were observed upon photoirradiation at any wavelength in hexane or methanol solutions. Considering the corresponding perfluorocyclopentene derivative,¹² the reason was attributed to the nonplanarity of the structure of **2o** due to the steric repulsion between the two hydrogen atoms on the azulene and thiophene rings (Figure S3, Supporting Information). Kawai et al. have proposed that the coplanarity of aromatic rings is important in enhancing photoreactivity and achieved a cyclization quantum yield of 1.0 by introducing thiazole units which are effective for fixing the conformation of the three aromatic rings by intramolecular hydrogen bonding.¹³ Therefore, the difference of the photoreactivity of **1o** and **2o** is attributed to the planarity of the open-ring isomer structures due to intramolecular hydrogen bonding.

The photochemical quantum yield for ring closing was measured at wavelengths corresponding to the two absorption bands to ascertain the wavelength dependence of the cyclization of **1o**. The cyclization quantum yield (ϕ_c) at 313

nm, which corresponds to the excitation from S_0 to the higher singlet state, was measured to be 1.7×10^{-3} , which is much smaller than that of the corresponding perfluorocyclopentene analogue (0.32 (at 313 nm) of 1,2-bis(5-methyl-2-phenylthiazol-4-yl)perfluorocyclopentene).^{10a} In contrast, no changes in the absorption spectrum was observed upon excitation into the $S_0 \rightarrow S_1$ band (635 nm, 2.45 mW) for 60 h. This shows that the cyclization quantum yield is estimated to be $\ll 10^{-6}$ and apparently zero. From these results, the photocyclization reaction of **1o** was controlled by the selection of the wavelength of excitation. For the cycloreversion reaction, the quantum yield (ϕ_o) was determined to be 1.0×10^{-4} at 492 nm. The value was also much smaller than that of the perfluorocyclopentene analogue (0.02 at 492 nm).^{10a}

To understand why the photochromic quantum yields are so low, we analyzed the geometries (Figure 2) and electronic

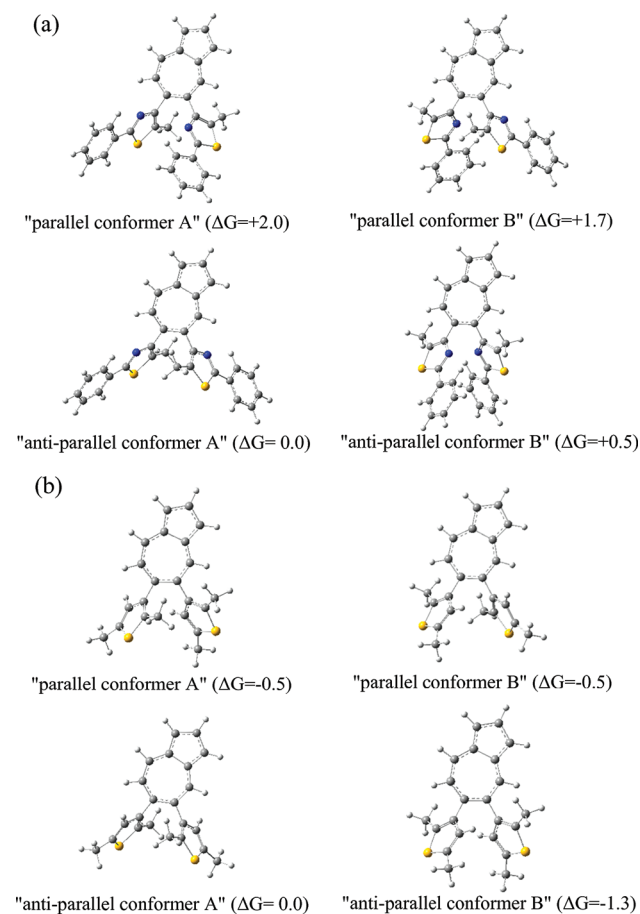


Figure 2. Optimized structures of conformers for **1o** (a) and **2o** (b). Colored spheres represent atoms: yellow = sulfur, blue = nitrogen, gray = carbon, white = hydrogen. For notations of "parallel" and "anti-parallel" see text. "G" in parentheses indicates the Gibbs free energy (kcal/mol) relative to that of "anti-parallel conformer A". Geometries are optimized by B3LYP/6-31G(d) in hexane solvent with PCM. Free energies are obtained at 298.15 K.

structures (Figure 3) using density functional theory with the B3LYP¹⁴ exchange-correlation functional and with the 6-31G(d) basis set¹⁵ in Gaussian 09.¹⁶ (It has been reported that the valence excitation wavelengths given by the TD-B3LYP method agree with the experimental UV/vis spectrum better than those by the long-range corrected (TD-CAM-B3LYP)¹⁷ and meta-GGA(TD-M06-2X)¹⁸ functionals.¹⁹ We also assessed

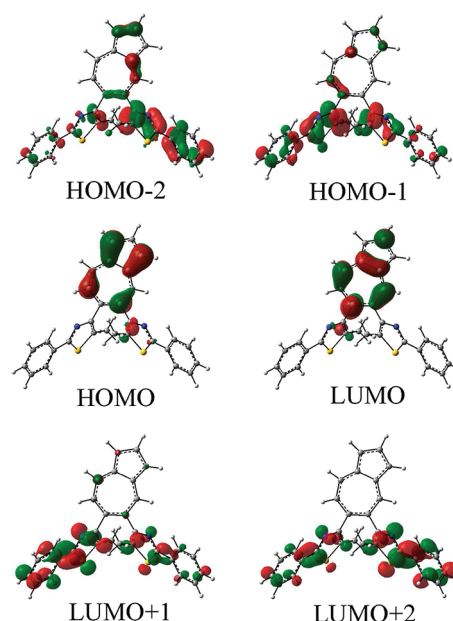


Figure 3. Kohn-Sham orbitals of **1o** obtained at the S_0 structure. The S_1 - S_{10} TDDFT excitations are expressed mainly by singly excitations from HOMO-2, HOMO-1, or HOMO to LUMO, LUMO+1, or LUMO+2. Colored spheres represent each atom, similar to Figure 2. Geometries are optimized by B3LYP/6-31G(d) in hexane solvent with PCM.

the accuracy of excitation energies by the B3LYP method in other diarylethene systems and found the excitation energies by TD-B3LYP was quite accurate.²⁰ We thus employed B3LYP in the following calculations. For **1o**, the excitation energies by CAM-B3LYP and M06-2X are blue-shifted in comparison with those by B3LYP. See the Supporting Information for the excitation energies of **1o** by the CAM-B3LYP and M06-2X functionals.) The effect of hexane solvent was taken into account by polarizable continuum model (PCM).²¹

The relative free energies of each conformer are shown in parentheses of Figure 2. The notations "parallel" and "anti-parallel" represent the conformers distinguished by the geometry (rotational angle) of the two thiophene rings. Previous studies concerning diarylethene photochromes showed that interconversion between the two conformers is much slower than photocyclization,^{7,11} and photocyclization only occurs²² by the antiparallel conformer A in a conrotatory fashion because the distance between the two reactive carbon atoms of the antiparallel conformer B is larger than 0.4 nm, and therefore, no possibility exists for the cyclization reaction.²³ In the case of **2o**, the free energy of "anti-parallel conformer A" is higher than those of the other conformers; on the other hand, in the case of **1o** it is the lowest. Therefore, considering the Boltzmann populations of the conformers which can undergo ring closure, the calculations rationalize that cyclization can be expected in **1o** but not in **2o**.

We measured the fluorescence quantum yield (Q_F). The fluorescence spectra of **1o** and **2o** indicate they fluoresce from the S_2 state, as is the case of the azulene molecule. The fluorescence quantum yields of **1o** and **2o** were determined to be 0.002 and 0.005, respectively, by comparison with the spectrum of rhodamine B (see the Supporting Information). Here, the fluorescence quantum yield and the cyclization quantum yield are given by $Q_F = k_R \tau$ and $Q_{clo} = k_{clo} \tau$, respectively, where an excited state lifetime is given by $\tau = (k_R +$

$k_{\text{NR}} + k_{\text{clo}})^{-1}$, the radiative decay rate is k_{R} , the nonradiative decay rate is k_{NR} , and the cyclization reaction rate is k_{clo} . Considering that the fluorescence emits from the S_2 state and that the cyclization reaction might start not from the S_2 (charge transfer ($\text{Az} \rightarrow \text{DAE}/\text{DAE} \rightarrow \text{Az}$)) state but from a higher S_n (intra-DAE excitation) state, which will be explained later, no cyclization reaction from S_2 with the small Q_{F} means that $k_{\text{NR}}(S_2 \rightarrow S_1)$ is very large and no fluorescence from $S_n (n > 2)$ with the small Q_{clo} indicates that $k_{\text{NR}}(S_n (n > 2) \rightarrow S_1)$ is quite large.

The second question concerns why the quantum yield of the cyclization of **1o** depends on the excitation wavelength. We calculated the vertical excitation energies of **1** as a function of the C–C distance of two reactive carbon atoms for the cyclization reaction.²⁴ Since the ground and excited states around the pericyclic minimum where HOMO and LUMO energies of DAE cross each other cannot be described by conventional (TD-)DFT methods, in other words the TDDFT analysis of the cyclization reaction is valid only from the FC region before a DAE 1B/2A conical intersection point which remains unknown in this study, in the following we quite roughly discuss only the initial stage of cyclization reaction path of **1** using TDDFT potential energy surfaces (PESs) along the C–C distance of two reactive carbon atoms.

Figure 4 shows the PESs of the ground state S_0 and the vertical excited states of S_1 – S_{10} . The excitation energies, the

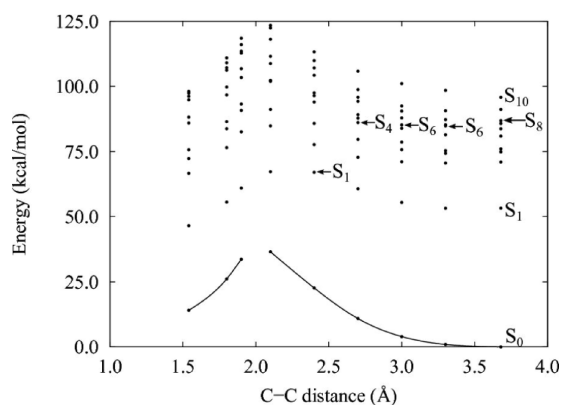


Figure 4. Potential energy surfaces of **1** along C–C distance (distance of two carbon atoms that form a single bond by photocyclization). Solid line shows energy of S_0 state, and each dot represents energy of S_1 – S_{10} vertically excited. Geometries are optimized by B3LYP/6-31G(d) in hexane solvent with PCM. Excitation energies are calculated by time-dependent DFT with B3LYP/6-31G(d) and with PCM.

oscillator strengths, and the Kohn–Sham (KS) orbitals at the equilibrium geometry of **1o** in the ground state (3.67 Å in Figure 4) as well as at the C–C distances with 3.0, 2.7, and 2.4 Å are summarized in Tables S1–S4 of the Supporting Information. The KS orbitals in Tables S1–S4 are shown in Figures 3 and 5 and also Figures S4 and S5 in the Supporting Information. We found that the S_1 Franck–Condon (FC) state of **1o** is mainly due to the HOMO–LUMO transition and localized around the azulene ring (Figure 3). Since the character of the S_1 state of **1o** primarily corresponds to that of the S_1 state (mainly due to the HOMO–LUMO transition) of azulene (Figure 6) whose S_1 lifetime is very short (around 1 ps),⁴ the S_1 lifetime of **1o** is considered too short to overcome the energy barrier of the S_1 state for the cyclization reaction (around 14.0 kcal/mol shown in Figure 4). Regarding the S_n

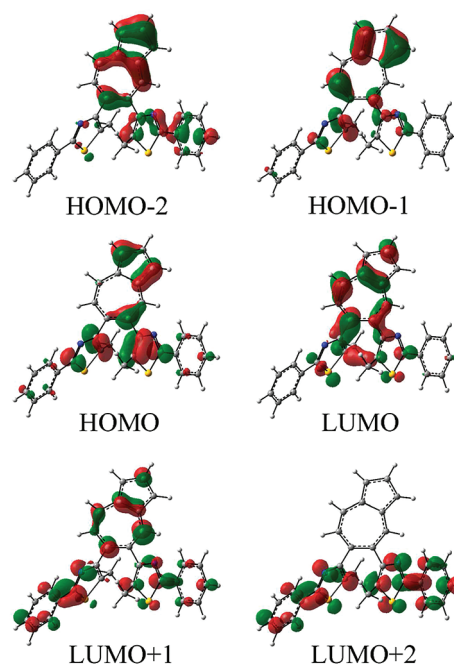


Figure 5. Kohn–Sham orbitals of **1** obtained at 2.4 Å of C–C distance. The S_1 – S_{10} TDDFT excitations are expressed mainly by singly excitations from HOMO-2, HOMO-1, or HOMO to LUMO, LUMO+1, or LUMO+2. Colored spheres represent each atom, similar to Figure 2. Geometries are optimized by B3LYP/6-31G(d) in hexane solvent with PCM.

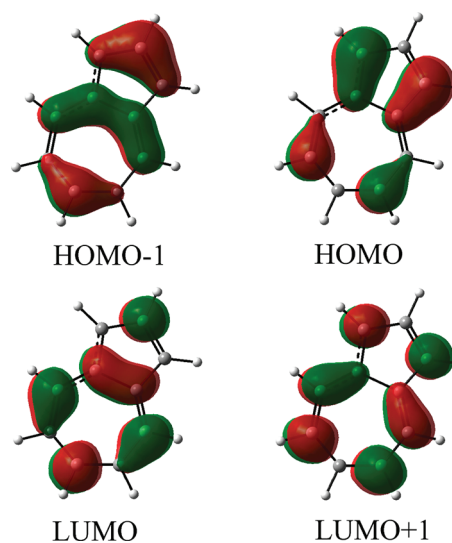


Figure 6. Kohn–Sham orbitals of azulene molecule. These orbitals become occupied/unoccupied by the electronic excitation to fluorescence-emitting S_2 state. Geometries are optimized by B3LYP/6-31G(d) in hexane solvent with PCM.

states above S_1 , roughly characterized, the S_2 – S_6 states have charge transfer (CT) ($\text{Az} \rightarrow \text{DAE}/\text{DAE} \rightarrow \text{Az}$) excitation character and the S_7 – S_8 states have intra-DAE excitation character in the TD-B3LYP results. Both S_7 and S_8 states, whose energies are very close to each other, contain a HOMO-1→LUMO+2 excitation configuration which corresponds to a HOMO→LUMO excitation (1B state) of the DAE part and leads to a cyclization reaction. Following the TD-B3LYP results, it is considered that the cyclization reaction of **1o** starts not from the CT ($\text{Az} \rightarrow \text{DAE}/\text{DAE} \rightarrow \text{Az}$) excitation but from the intra-

DAE excitation of the S_7 and/or S_8 state. Considering that the TD-B3LYP amplitude of the HOMO-1→LUMO+2 excitation in the S_8 state is larger than that in the S_7 state, we assumed that the cyclization reaction starts from the S_8 FC state in the following. (The excited state characters of **1o** at the TD-CAM-B3LYP and TD-M06-2X levels are shown in Tables S5 and S6 of the Supporting Information.)

Now we will see the reactive C–C bond length dependency of energies and characters of the excited states to make a qualitative discussion about the initial stage of the cyclization reaction path of **1o**. Excited states which has a character similar to the S_8 FC state of **1o** appear in the excited state S_6 (HOMO-1–LUMO+1 transition) at C–C distances of 3.3 and 3.0 Å (Figures 4 and S4, Supporting Information). Then the excited states start to mix with the azulene localized S_1 state, as seen in the S_4 state (HOMO–LUMO+2 transition) at a C–C distance of 2.7 Å (Figure S5, Supporting Information) and finally reaches the S_1 state (HOMO–LUMO transition) at a C–C distance of 2.4 Å with a significant mixture of the azulene S_1 state but with the C–C bond character of the LUMO orbital (Figure 5). Thus, we expect that the cyclization reaction will proceed through the diabatic potential energy surface indicated by the arrows after the initial excitation to the S_8 state in Figure 4. To further confirm this view, we calculated the forces of **1o** at the S_8 FC state and found that they are directed toward the cyclization reaction (Table 1 and Figure 7). (We previously

Table 1. Forces in Internal Coordinate (Hartree/Bohr or Hartree/Radian) for Atoms (N1) of **1o** at the S_8 State with S_0 -Optimized Structure^a

N1	N2	length/force	N3	angle/force	N4	dihedral/force
C5	C1	+1.497	C3	+112.908	C4	−174.912
		−0.008598		+0.018234		+0.002191
C6	C5	+1.377	C1	+125.361	C3	+116.838
		+0.041416		−0.069662		+0.015019
C7	C2	+1.496	C1	+120.147	C3	+170.477
		−0.002836		−0.021733		+0.014336
C8	C7	+1.377	C2	+125.468	C3	−62.337
		+0.029992		−0.055300		+0.010420

^aN2, N3, and N4 are the atoms for bond length (N1–N2), bond angle (N1–N2–N3), and dihedral angle (N1–N2–N3–N4). Positive (negative) force operates to increase (decrease) the corresponding internal coordinate. Labels for each atom (C1–C8) correspond to that of Figure 7. Those values are obtained by B3LYP/6-31G(d) in hexane solvent with PCM.

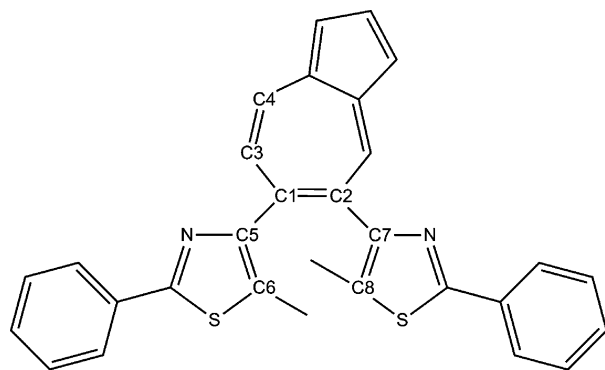


Figure 7. Molecular Structure of **1o**. Labels for carbon atoms (C1–C8) correspond to that of Table 1.

showed that the force of the closed-ring isomer of diarylethene at the Franck–Condon state is correlated with the cyclization reaction.²⁵)

In conclusion, we synthesized diarylethene derivatives with an azulene ring as the ethene moiety, and a derivative having thiazole rings showed photochromism. By introducing the azulene ring, the diarylethene gains several excited states, and the cyclization reaction proceeds from a higher excited state but not from the lowest state. Theoretical calculations showed that the cyclization reaction proceeded through a diabatic potential energy surface from higher electronic states, which are similar to the excited states of the diarylethenes, and the S_1 state and the lower S_n states correspond to the S_1 state of azulene and the CT(Az→DAE/DAE→Az) states, respectively. A photochromic system with such selective excitation will be useful for optical logic gate and nondestructive readout materials.

EXPERIMENTAL SECTION

General Methods. All solvents used were reagent grade and were distilled before use. ¹H NMR spectra were recorded at ambient temperature. Chemical shifts are denoted in δ units (ppm) relative to the solvent signals CHCl₃ (¹H NMR: δ = 7.24 ppm, ¹³C: δ = 77.0 ppm). Mass spectra (FAB-MS) were obtained by using 3-nitrobenzyl alcohol and glycerol as the matrix. UV light was irradiated by a hand lamp SPECTROLINE Model EB-280C/J (λ : 312 nm). Visible light was irradiated by a 500 W Xe-arc lamp (USHIO SX-UI501XQ). For the absorption spectral measurements, optical cells with 1 cm light pass lengths were used for the absorption spectral measurement of the solutions. A diode laser (Neoark DMSH-3S, λ 635 nm, 2.45 mW) was applied for the irradiation of the S_0 to S_1 excitation of a diarylethene derivative in hexane solution.

Synthesis. 5,6-Bis(5-methyl-2-phenylthiazol-4-yl)azulene (**1o**). To a THF anhydrous solution (20 mL) containing 1.39 g (5.46 mmol) of 4-bromo-5-methyl-2-phenylthiazole (**3**)^{10a} was gradually added 4.10 mL (6.55 mmol) of 1.6 N *n*-BuLi hexane solution at −78 °C in an argon gas atmosphere followed by stirring for 1 h at that temperature. Then, 1.77 mL (6.55 mmol) of B(OBu)₃ was added and the mixture stirred at that temperature for 30 min, followed by stirring at room temperature. To the reaction mixture were added 5,6-dibromoazulene (**4**) (0.60 g, 2.10 mmol), Pd(PPh₃)₄ (0.14 g, 0.126 mmol), 10.5 mL of 2 M Na₂CO₃ aqueous solution, and 20 mL of THF, and then the solution was heated by microwave. The heating was carried out by using a microwave reactor (Shikoku Instrumentation Co., Ltd.; ZMW-023) for 2 h with divided irradiation periods of 1 min. In the middle period, additional Pd(PPh₃)₄ (0.073 g, 0.063 mmol) was added. After the reaction was over, 50 mL of water and 20 mL of ether were added, and the organic layer was separated. The water layer was extracted with ether (30 mL × 3), and the combined organic layer was dehydrated over sodium sulfate anhydrous. After the sodium sulfate was filtered off, the solvent was evaporated then the residue was purified by column chromatography (hexane/ethyl acetate = 95:5) to obtain 0.30 g (0.63 mmol) of a deep-blue colored oil. Recrystallization from the hexane solution at 5 °C gives 0.076 g of deep-colored crystals of **1o** in 7.6% yield.

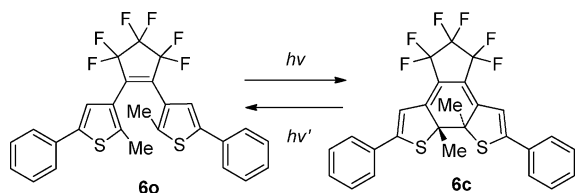
1o. Mp: 138.1–139.9 °C. ¹H NMR (400 MHz, CDCl₃) δ : 2.25 (s, 3H), 2.29 (s, 3H), 7.32–7.35 (m, 6H), 7.43 (d, J = 9.6 Hz, 1H), 7.47 (d, J = 3.7 Hz, 2H), 7.79–7.84 (m, 4H), 7.97 (t, J = 3.8 Hz, 1H), 8.42 (d, J = 9.6 Hz, 1H), 8.62 (s, 1H). ¹³C NMR (100 MHz, CDCl₃) δ : 12.4*, 12.5*, 118.9, 120.0, 125.7, 126.3*, 126.4*(4C), 128.9 (4C), 129.56*, 129.62*(2C), 129.8*, 130.1*, 133.9*, 134.0*, 135.4, 138.0, 139.2*, 139.3*, 139.6(2C), 144.2(2C), 155.15*, 155.23*, 163.0*, 163.3* (signals with marked with an asterisk are split due to atropisomerization.¹⁰ Underlines with (*n*C) indicate the total number of carbon atoms for split lines is *n*). IR (KBr): 753, 830, 1140, 1402, 1440, 1577, 2856, 2916, 2944 cm^{−1}. Anal. Calcd for C₃₀H₂₂N₂S₂: C, 75.91; H, 4.67; N, 5.90. Found: C, 76.09; H, 4.70; N, 5.84.

5,6-Bis(2,5-dimethylthiophene-3-yl)azulene (2o). To a THF anhydrous solution (10 mL) containing 0.83 g (3.50 mmol) of 3-iodo-2,5-dimethylthiophene (**5**)²⁶ was gradually added 3.07 mL (4.90 mmol) of 1.6 N *n*-BuLi hexane solution at -78 °C in an argon gas atmosphere followed by stirring for 1 h at that temperature. Then, 1.23 mL (4.55 mmol) of B(OBu)₃ was added and the mixture stirred at that temperature for 30 min, followed by additional stirring for 2 h at room temperature. To the reaction mixture were added 5,6-dibromoazulene (**4**) (0.40 g, 1.40 mmol), Pd(PPh₃)₄ (0.194 g, 0.168 mmol), 7.0 mL of 2 M Na₂CO₃ aqueous solution, and 10 mL of THF, and then the solution was refluxed for 14 h. After the reaction was over, 20 mL of water and 10 mL of ether was added, and the organic layer was separated. The water layer was extracted with ether (10 mL × 3), and the combined organic layer was dehydrated over sodium sulfate anhydrous. After the sodium sulfate was filtered off, the solvent was evaporated and then the residue was purified by column chromatography (hexane/ethyl acetate = 95:5) to obtain 0.10 g (0.29 mmol) of **2o** as a deep-blue colored oil in 20.5% yield.

2o. ¹H NMR (400 MHz, CDCl₃) δ: 2.14 (s, 3H), 2.17 (s, 3H), 2.31 (s, 3H), 2.33 (s, 3H), 6.25 (s, 1H), 6.29 (s, 1H), 7.18 (d, *J* = 10.4 Hz, 1H), 7.34 (d, *J* = 3.6 Hz, 1H), 7.38 (d, *J* = 2.8 Hz, 1H), 7.89 (t, *J* = 3.6 Hz, 1H), 8.28 (d, *J* = 10.4 Hz, 1H), 8.37 (s, 1H). ¹³C NMR (100 MHz, CDCl₃) δ: 13.9, 14.0, 15.08, 15.15, 117.8, 118.8, 126.0, 127.7*, 128.1*, 131.7, 134.5(2C), 134.6, 137.3, 138.4, 138.8*, 140.1(2C), 141.4*, 142.0*, 146.6(2C). EI-MS (*m/z*): 348 (M⁺). HRMS: calcd for C₂₂H₂₀S₂ 348.1006, found 348.1008. IR (KBr): 601, 689, 760, 848, 971, 1241, 1398, 1435, 1462, 1501, 1514, 1577, 2852, 2916, 3020, 3061 cm⁻¹.

Computational Method. Geometries were optimized by using B3LYP/6-31G(d) with a polarizable continuum model (PCM) to consider hexane solvent. Free energies were obtained at 298.15 K. Excitation energies were calculated by using time-dependent DFT with B3LYP/6-31G(d) and with PCM under the Franck–Condon conditions. All calculations were performed by using Gaussian 09.¹⁶

Photochromic Quantum Yield Measurement. The quantum yields of photoinduced cyclization and cycloreversion reactions of **1** were determined in hexane by measuring the rate of isomerization in the initial stage of the reactions, comparing the reaction yields of **1** against diarylethene **6**.²⁷ The absorbance of the compounds at the irradiating wavelength was controlled at 0.4.



■ ASSOCIATED CONTENT

■ Supporting Information

¹H NMR spectral changes of diarylethene **1** by alternative irradiation with UV and visible light, the temperature dependence of the thermal fading of **1c** in hexane, Kohn–Sham orbitals of **1**, calculated excitation energy, oscillator strength, and the change of orbital occupation for the electronic vertical excitation of **1o**, **1c**, **2o**, and azulene, Cartesian coordinates of **1o**, **1c**, **2o**, and azulene, calculated free energies of **1o** and **2o**, calculated potential energies of **1o**, **1c**, and azulene, fluorescence emission spectra, NMR spectra, elemental analysis, and HRMS of new compounds. This material is available free of charge via the Internet at <http://pubs.acs.org/>.

■ AUTHOR INFORMATION

Corresponding Authors

*(T.K.) E-mail: tkoba@rsi.co.jp.

*(S.N.) E-mail: snakamura@riken.jp.

*(K.U.) Tel: +81-77-543-7462. Fax: +81-77-543-7483. E-mail: uchida@rins.ryukoku.ac.jp.

Notes

The authors declare no competing financial interest.

■ ACKNOWLEDGMENTS

This study was partially supported by Grants-in-Aids for Scientific Research on Priority Area “New Frontiers in Photochromism (No. 471)” from the Ministry of Education, Culture, Sports, Science, and Technology (MEXT), Japan. All calculations were performed on TSUBAME, a supercomputer at the Tokyo Institute of Technology.

■ REFERENCES

- (1) (a) Feringa, B. L.; Wesley, R. B., Ed. *Molecular Switches*; Wiley-VCH: Weinheim, 2011. (b) Irie, M.; Fukaminato, T.; Sasaki, T.; Tamai, N.; Kawai, K. *Nature* **2002**, *420*, 759–760. (c) Liddell, P. A.; Kodis, G.; Moore, A. L.; Moore, T. A.; Gust, D. *J. Am. Chem. Soc.* **2002**, *124*, 7668–7669. (d) Endtner, J. M.; Effenberger, F.; Hartschuh, A.; Port, H. *J. Am. Chem. Soc.* **2000**, *122*, 3037–3046.
- (2) (a) Lloyd, D. *Nonbenzenoid Conjugated Carbocyclic Compounds*; Elsevier: Amsterdam, 1984; pp 352–377. (b) Heritage, J. P.; Penzkofer, A. *Chem. Phys. Lett.* **1976**, *44*, 76–81. (c) Murata, S.; Iwanaga, C.; Toda, T.; H. Kokubun, H. *Ber. Buns. Phys. Chem.* **1972**, *76*, 1176–1183.
- (3) Kasha, M. *Disc. Faraday Soc.* **1950**, *9*, 14–19.
- (4) (a) Beer, M.; Longuet-Higgins, H. C. *J. Chem. Phys.* **1955**, *23*, 1390–1391. (b) Bearpark, M. J.; Bernardi, F.; Clifford, D. S.; Olivucci, M.; Robb, M. A.; Smith, B. R.; Vreven, T. *J. Am. Chem. Soc.* **1996**, *118*, 169–175. (c) Foggi, P.; Neuwahl, F. V. R.; Moroni, L.; Salvi, P. R. *J. Phys. Chem. A* **2003**, *107*, 1689–1696. (d) Murakami, A.; Kobayashi, T.; Goldberg, A.; Nakamura, S. *J. Chem. Phys.* **2004**, *120*, 1245–1252. (e) Michl, J.; Thulstrup, E. W. *Tetrahedron* **1976**, *32*, 205–209. (f) Matsuda, H.; Nagasawa, Y.; Miyasaka, H.; Okada, T. *J. Photochem. Photobiol. A* **2003**, *156* (1–3), 69–75.
- (5) Karatsu, T.; Kitamura, A.; Arai, T.; Sakuragi, H.; Tokumaru, K. *Bull. Chem. Soc. Jpn.* **1994**, *67*, 1674–1679.
- (6) (a) Irie, M. *Chem. Rev.* **2000**, *100*, 1683–1684. (b) Irie, M.; Uchida, K. *Bull. Chem. Soc. Jpn.* **1998**, *71*, 985–996.
- (7) Miyasaka, H.; Nobuto, T.; Itaya, A.; Tamai, N.; Irie, M. *Chem. Phys. Lett.* **1997**, *269*, 281–285.
- (8) Fukaminato, T.; Doi, T.; Tamaoki, N.; Okuno, K.; Ishibashi, Y.; Miyasaka, H.; Irie, M. *J. Am. Chem. Soc.* **2011**, *133*, 4984–4990.
- (9) Lu, Y.; Lemal, D. M.; Jasinski, J. P. *J. Am. Chem. Soc.* **2000**, *122*, 2440–2445.
- (10) (a) Uchida, K.; Ishikawa, T.; Takeshita, M.; Irie, M. *Tetrahedron* **1998**, *54*, 6627–6638. (b) Takami, S.; Kuroki, L.; Irie, M. *J. Am. Chem. Soc.* **2007**, *129*, 7319–7326. (c) Iwata, S.; Ishihara, Y.; Qian, C. P.; Tanaka, K. *J. Org. Chem.* **1992**, *115*, 10292–10297. (d) Nakagawa, T.; Hasegawa, Y.; Kawai, T. *J. Phys. Chem. A* **2008**, *112*, 5096–5103. (e) Li, Z.-X.; Liao, L.-Y.; Sun, W.; Xu, C.-H.; Zhang, C.; Fang, C.-J.; Yan, C.-H. *J. Phys. Chem. C* **2008**, *112*, 5190–5196.
- (11) Uchida, K.; Nakayama, Y.; Irie, M. *Bull. Chem. Soc. Jpn.* **1990**, *63*, 1311–1315.
- (12) Irie, M.; Lifka, T.; Kobatake, S.; Kato, N. *J. Am. Chem. Soc.* **2000**, *122*, 4871–4876.
- (13) Fukumoto, S.; Nakashima, T.; Kawai, T. *Angew. Chem., Int. Ed.* **2011**, *50*, 1565–1568.
- (14) (a) Becke, A. D. *J. Chem. Phys.* **1993**, *98*, 5648. (b) Becke, A. D. *Phys. Rev. A* **1988**, *38*, 3098. (c) Lee, C.; Yang, W.; Parr, R. G. *Phys. Rev. B* **1988**, *37*, 785.
- (15) (a) Hehre, W. J.; Ditchfield, R.; Pople, J. A. *J. Chem. Phys.* **1972**, *56*, 2257–2261. (b) Hariharan, P. C.; Pople, J. A. *Theor. Chim. Acta* **1973**, *28*, 213–222. (c) Francl, M. M.; Pietro, W. J.; Hehre, W. J.; Binkley, J. S.; Gordon, M. S.; DeFrees, D. J.; Pople, J. A. *J. Chem. Phys.* **1982**, *77*, 3654–3665.

- (16) Gaussian 09, Revision A.2, Frisch, M. J. et al. Gaussian, Inc., Wallingford CT, 2009.
- (17) Yanai, T.; Tew, D. P.; Handy, N. C. *Chem. Phys. Lett.* **2004**, *393*, 51–57.
- (18) Zhao, Y.; Truhlar, D. G. *Theo. Chem. Acc.* **2008**, *120*, 215–241.
- (19) Jacquemin, D.; Wathelet, V.; Perpète, E. A.; Adamo, C. J. *Chem. Theor. Comput.* **2009**, *5*, 2420–2435.
- (20) (a) Yokojima, S.; Matsuda, K.; Irie, M.; Murakami, A.; Kobayashi, T.; Nakamura, S. *J. Phys. Chem. A* **2006**, *110*, 8137–8143. (b) Yokojima, S.; Kobayashi, T.; Shinoda, K.; Matsuda, K.; Higashiguchi, K.; Nakamura, S. *J. Phys. Chem. B* **2011**, *115*, 5685–5692.
- (21) (a) Scalmani, G.; Frisch, M. J. *J. Chem. Phys.* **2010**, *132*, 114110. (b) Imbrota, R.; Barone, V.; Scalmani, G.; Frisch, M. J. *J. Chem. Phys.* **2006**, *125*, 054103.
- (22) Uchida, K.; Guillaumont, D.; Tsuchida, E.; Mochizuki, G.; Irie, M.; Murakami, A.; Nakamura, S. *THEOCHEM* **2002**, *579*, 115–120.
- (23) Kobatake, S.; Uchida, K.; Tsuchida, E.; Irie, M. *Chem. Commun.* **2002**, 2804–2805.
- (24) The geometry at each C–C bond distance point was obtained by S0 optimization with the C–C bond constraint.
- (25) Nakamura, S.; Kanda, K.; Guillaumont, D.; Uchida, K.; Irie, M. *Nonlinear Opt.* **2000**, *26*, 201–205.
- (26) Kobatake, S.; Yamada, T.; Uchida, K.; Kato, N.; Irie, M. *J. Am. Chem. Soc.* **1999**, *121*, 2380–2386.
- (27) (a) Irie, M.; Sakemura, K.; Okinaka, M.; Uchida, K. *J. Org. Chem.* **1995**, *60*, 8305–8309. (b) Yokoyama, Y.; Kurita, Y. *Nippon Kagaku Kaishi* **1992**, 998. (c) Yokoyama, Y.; Kurita, Y. *Synth. Org. Chem. Jpn.* **1991**, *49*, 364.

■ NOTE ADDED AFTER ASAP PUBLICATION

This paper was published ASAP on March 20, 2012. The Supporting Information file was updated. The revised paper was reposted on March 23, 2012.